Available online at ScienceDirect

Nuclear Engineering and Technology

journal homepage: www.elsevier.com/locate/net

Original Article

Measurement of Photo-Neutron Dose from an 18-MV Medical Linac Using a Foil Activation Method in View of Radiation Protection of Patients

Haluk Yücel [a,*], *İbrahim Çobanbaş* [b], *Asuman Kolbaşı* [a], *Alptuğ Özer Yüksel* [a], *and Vildan Kaya* [b]

[a] *Ankara University, Institute of Nuclear Sciences, Tandogan, Ankara 06100, Turkey*
[b] *Süleyman Demirel University, School of Medicine, Department of Radiation Oncology, Çünür, Isparta 32260, Turkey*

ARTICLE INFO

Article history:
Received 27 October 2014
Received in revised form
30 October 2015
Accepted 7 November 2015
Available online 8 December 2015

Keywords:
Dose
Foil activation
Neutron
Patient
Radiotherapy
Radiation protection

ABSTRACT

High-energy linear accelerators are increasingly used in the medical field. However, the unwanted photo-neutrons can also be contributed to the dose delivered to the patients during their treatments. In this study, neutron fluxes were measured in a solid water phantom placed at the isocenter 1-m distance from the head of an 18-MV linac using the foil activation method. The produced activities were measured with a calibrated well-type Ge detector. From the measured fluxes, the total neutron fluence was found to be $(1.17 \pm 0.06) \times 10^7$ n/cm^2 per Gy at the phantom surface in a 20×20 cm^2 X-ray field size. The maximum photo-neutron dose was measured to be 0.67 ± 0.04 mSv/Gy at $d_{max} = 5$ cm depth in the phantom at isocenter. The present results are compared with those obtained for different field sizes of 10×10cm^2, 15×15cm^2, and 20×20cm^2 from 10-, 15-, and 18-MV linacs. Additionally, ambient neutron dose equivalents were determined at different locations in the room and they were found to be negligibly low. The results indicate that the photo-neutron dose at the patient position is not a negligible fraction of the therapeutic photon dose. Thus, there is a need for reduction of the contaminated neutron dose by taking some additional measures, for instance, neutron absorbing-protective materials might be used as aprons during the treatment.

1. Introduction

Several types of accelerators are increasingly used for medical purposes. Today, as a suitable photon source, linear accelerators (linacs) are commonly employed in radiotherapy to treat cancer. Modern medical linacs can be used in two distinct operation modes: electron mode and photon mode. In electron mode, primary electrons are used for treatment, but

* *Corresponding author.*
E-mail address: haluk.yucel@ankara.edu.tr (H. Yücel).
http://dx.doi.org/10.1016/j.net.2015.11.003

in photon mode, photons are used for treatment. In the photon mode operation of a linac, unwanted neutrons are created during the radiation therapy by photonuclear reactions (γ,n) from the interfering elements in the accelerator head (target, field-flattening filters, and beam collimators) and other structural materials. In the photon mode, higher energy photons above the threshold of the (γ,n) photonuclear reaction of the elements such as W and Pb used in the treatment head can interact with nuclei of those high-Z materials and liberate fast neutrons. If the photon energy in a (γ,n) reaction is greater than the binding energy of the last neutron in the nucleus, then the threshold energy E_{th} can be calculated to be 7.41 MeV for the $^{184}W(\gamma,n)\,^{183}W$ reaction and 7.19 MeV for the $^{186}W(\gamma,n)\,^{185}W$ reaction when a tungsten target is used in the head [1].

It is very likely that these neutrons can scatter throughout the treatment room and reach the patient position. Thus even small neutron fluxes may have harmful effects on the patient since neutrons have a high radiation quality factor compared with those of x/γ radiations for the dose deposited in tissue or organs. However, the body related protection quantities, e.g., equivalent dose and effective dose are not measurable in practice. Instead, operational quantities such as $H_p(10)$, $H_p(0.07)$, and $H^*(10)$ are used for the assessment of effective dose or mean equivalent doses in tissue or organs [2]. For instance, an individual dosimeter worn on the body gives the dose equivalent to $H_p(10)$, which represents the dose at a depth, d = 10 mm below a specified point on the human body. Additionally, the operational quantity, $H^*(10)$, was used for estimating the ambient dose equivalent values from the neutron fluences in some locations of radiotherapy and operator rooms. When high photon doses of about 50 Gy in total are given at the isocenter position (0,0,0), a significant amount of neutrons are generated thorough photonuclear reactions. Therefore, it is worth noting that although the treatment head of linac was shielded to a large extent by the massive shielding, photon leakage is still much more abundant than the neutron flux. However, in recent years, higher energy linacs (6–18 MV) are commonly used in radiotherapy. Often, either 6 MV or 18 MV in linacs is more preferable for cancer treatment. As a result, the production of unwanted fast neutrons due to the increase in photon energy can contaminate the therapeutic beam and also give a non-negligible contribution to the patient dose [3]. The knowledge of the extra dose due to photoneutrons in the vicinity of the patient position is an important issue in radiological protection of patients. Thus, this dose information might be used for taking additional protective measures for reduction of unwanted neutron doses.

In high-energy photon beams in radiotherapy, the measurement of neutron fluxes and the corresponding absorbed dose is especially difficult due to the large ratio of photons to neutrons and the lack of knowledge about neutron energy spectra. Photons interfere through (γ,n) reactions in the detector and through pulse pile-up problems in the detectors which employ electronic pulse mode measurements. The responses of neutron detectors depend mainly on incident neutron energy, and thus fluence-to-dose conversion factors vary strongly with incident neutron energy [4]. Further, one requires knowledge of the neutron energy spectra which is difficult to obtain for fluence-to-dose

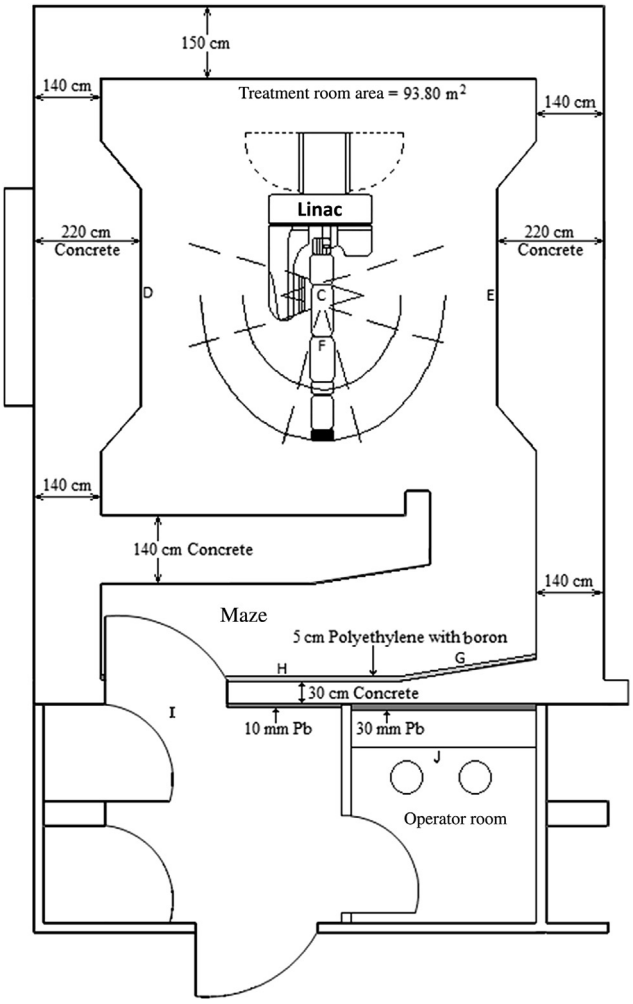

Fig. 1 – A schematic view of a Varian Clinac DHX linac and foil locations in treatment room. The letters A–J denote eight gold foils where they are placed in operator and treatment rooms.

conversion factors. In our literature survey, BF_3 proportional counters were used as an active detector to measure neutron fluence at about 4.6×10^5 n/cm^{-2} per Gy–X-ray dose using a Siemens 18-MV accelerator [5]. Suitable thermoluminescent dosimeters were also used to deduce the neutron contribution [6]. However, passive detectors such as activation detectors are good alternatives for accurate measurement of thermal and epithermal neutron fluxes inside the treatment room [4]. The neutron activation technique with use of indium foils was employed to measure thermal neutron flux in various locations in a treatment room with the use of 10- and 15-MV linacs [7]. Since the foil activation technique is a well-known and reliable method, it is a simple way to measure the thermal and epithermal components of the neutron flux in radiotherapy rooms. Its main advantage is that activation detectors are insensitive to photon radiation in a mixed field consisting of both neutrons and photons. These detectors also have some additional advantages such as their low cost and small sizes of the wire or foils, thus giving a better spatial resolution to deduce neutron doses. Nevertheless, the basic disadvantage of an

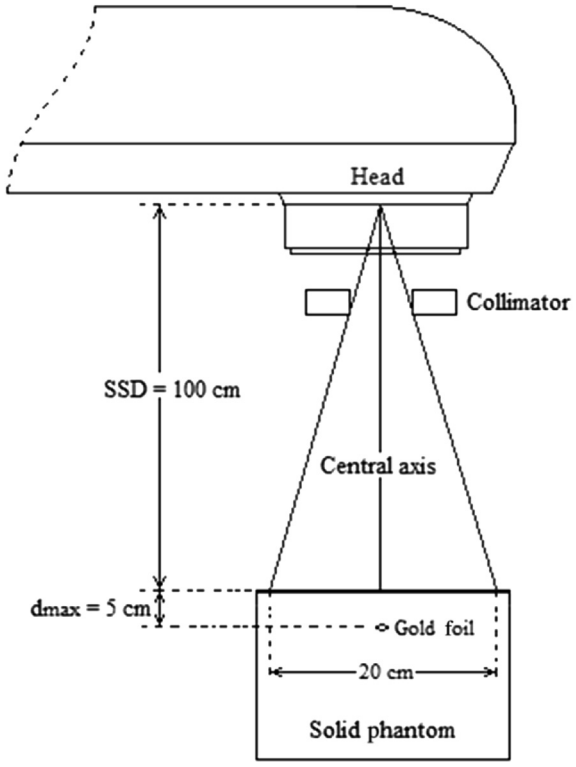

Fig. 2 – Irradiation geometry for foil activation detectors at isocenter on the z central axis. Isocenter is at the point (0,0,0) on the phantom. SSD, surface-to-source distance.

activation detector is that the activity produced in it has to be measured in a separate gamma counting system, which must be installed away from the treatment room. In this context, an ultimate monitor isotope, ^{197}Au, was previously used to measure the neutron fluence of 2.3×10^5 n/cm^2 per Gy-photon dose at a surface-to-source distance of 100 cm using an 18-MV accelerator [8]. This work aims to measure neutron fluxes (thermal plus epithermal neutrons) by using gold-foil activation and to determine the corresponding photo-neutron dose equivalent in mSv per Gy-photon dose at a patient position. Additionally, ambient dose equivalent values were estimated at different places in the treatment and operator rooms.

2. Materials and methods

2.1. *Description of linac facility and irradiation conditions*

A Varian Clinac DHX dual energy linear accelerator (Varian Medical Systems, Palo Alto, CA) in the Radiation Oncology Department of School of Medicine of Süleyman Demirel University in Isparta, Turkey was used in this work. It is capable of producing 6- and 18-MV X-ray beams and also electron beams with 6 MeV, 9 MeV, 12 MeV, 15 MeV, and 18 MeV energies for treatment purposes. Fig. 1 shows a schematic view of a radiotherapy room. The treatment room has a floor area of 93.80 m^2 and a height of 3.9 m. As primary barriers, the right wall is 2.2 m thick, the left wall is 2.8 m thick, and the back wall is 1.5 m thick concrete. The maze in the room was made of a 30-cm thick concrete wall lined with 5 cm of boron-loaded polyethylene and 3 cm of lead. A 1-cm thick steel was added the sliding door to slow down fast neutrons. The operator room is also shielded with a 30-cm thick concrete wall, covered with 3 cm of lead.

Gold foils are placed at different positions in the treatment room to measure neutron fluxes. The linac was operated at 18 MV photon mode and the gantry and collimator angle were positioned at 0° vertically oriented, pointing down at the floor. The accelerator isocenter is at position (0,0,0) in this work, as shown in Fig. 2. A water-equivalent solid slab phantom (RW3) was positioned at the isocenter. Each of the foils was interposed between phantom layers. The gold foil detectors with and without Cd shield cover were placed on the surface of the phantom at d = 0 cm and at depths of 5 cm and 10 cm from the surface. The standard RW3 phantom is considered to be water-equivalent in the energy ranges from 1.25 MeV (^{60}Co) to 25-MV linac photons and from 4- to 25-MeV electrons [9]. During the irradiation session, one bare and one Cd-covered gold foil were placed on the central axis and coirradiated in the RW3 solid phantom. The solid phantom surface was fixed at a surface-to-source distance of 100 cm. The maximum photon dose at 5 cm was measured to be 50.4 ± 0.6 Gy in the water phantom for a 20 × 20 cm^2 field size using an ionization chamber. Other photon doses were measured to be 41.9 ± 0.5 Gy at 10 cm, 34.7 ± 0.4 Gy at 15 cm, and 28.6 ± 0.3 Gy at 20 cm in the phantom for a time period of 748 seconds (about 12.5 minutes).

The foil irradiations were performed at the point of maximum photon dose of ~50.4 Gy (5,000 MU) accumulated during one irradiation session of 12.5 minutes. At the end of irradiation, the foils were transferred to the laboratory of the Institute of Nuclear Sciences in Ankara, Turkey for measurement of the activity produced in the foils by using a calibrated Ge detector.

2.2. *Description of the gamma-ray spectrometer*

The detector used is a p-type well Ge (Canberra Industries Inc., 800 Research Parkway, CT06450, USA; GCW4023) with a relative efficiency of 44.8% and a resolution of 2 keV at 1,332.5 keV. The Ge detector has a well with a 16-mm diameter and a 40-mm depth. It has a standard 10-cm thick lead shield graded by a 1-mm thick tin and 1.6-mm thick copper layers, jacketed by a 9.5-mm steel outer housing.

For the data acquisition, the preamplifier was connected to a spectroscopy amplifier (Canberra 2025) and then interfaced to a 16 K ADC/MCA analyzer (Canberra Multiport II) operating through Genie 2000 software (Canberra Industries Inc., 800 Research Parkway, CT06450, USA). The spectra were collected in 4,096 ADC/MCA channels by setting suitable adjustments [10].

Gold foils were measured using a 1-mm thick polystyrene tube in the well of the Ge detector. For this measurement geometry, the full-energy peak detection efficiency, ε_p for the 411.8 keV peak of ^{198}Au, was determined by means of ANGLE software (Advanced Quantative Gamma-Spectrometry

Table 1 – Decay and nuclear data for gold activation detector.

Characteristic properties	Value	Reference
Thermal neutron cross section, σ_0 (b)	98.7 (1)	[18]
Resonance integral cross section, I_0 (b)	1,550 (28)	[18]
Cadmium correction factor, F_{Cd}	0.991	[19]
Correction factor for departure from 1/v cross section behaviour, g_T	1.0051	[19]
Atomic weight, M (g/mol)	196.966569 (3)	[20]
Isotopic abundance of ^{197}Au, θ (%)	100	[20]
Half-life of ^{198}Au, $t_{1/2}$ (d)	2.6943 (3)	[21]
Correction factor for gamma self-attenuation in foil, F_s	1.009 (2)	[22]
Correction factor for true coincidence summing effects, F_c	0.996 (90)	[23]
Gamma emission probability of ^{198}Au, f_γ (%)	95.62 (6)	[21]
Peak energy of ^{198}Au, E_γ(keV)	411.80205 (17)	[21]

(ANGLE 3), Podgorica, Montenegro) [11] by using a reference efficiency curve. To do this, the point sources ^{22}Na, ^{57}Co, ^{54}Mn, ^{60}Co, ^{65}Zn, ^{109}Cd, ^{133}Ba, and ^{137}Cs (Eckert and Ziegler Inc., Valencia, CA, USA) were measured at a distance of 3 cm from the end-cap surface. The full-energy peak detection efficiency, ε_p, was also calculated using GESPECOR (Version 4.2) software (CID Media GmbH, Strurhweg 1, 63594 Hasselroth, Germany) that uses a Monte-Carlo simulation [12]. The resulting ε_p value for the 411.8 keV peak of ^{198}Au was found to be 0.298 ± 0.067 for a 12.7-mm diameter foil measured in the well of the detector.

Since the activity produced in each foil was high enough, they were left at least 1 day for high decaying activity, thus avoiding pulse pile-up and reducing dead time counting losses in the counting system. Thus, the measurement periods were chosen between 21 hours and 66 hours to obtain good statistics of the spectrum counts. The room background measurements were subtracted the peak area of interest.

2.3. *Neutron flux determination by gold foil activation method*

As a passive neutron detector, gold is well known and adopted as a reliable monitor to measure neutron fluxes in mixed radiation fields because of its good nuclear and decay properties, as given in Table 1. For instance, it behaves as a good 1/v-detector in the thermal neutron region with a relatively high neutron capture cross section of $\sigma_0 = 98.8 \pm 0.1$ b and resonance integral of $I_0 = 1{,}550 \pm 28$ b via ^{197}Au(n,γ)^{198}Au reaction. Most of the resonances of ^{197}Au occur at low energies, about 4.9 eV. Additionally, when gold is irradiated with neutrons, the total equivalent 2,200 m/s flux can be determined from the induced ^{198}Au activity by the following equation [13]:

$$\Phi_0 = \frac{1}{G_{th} g_T \sigma_0}\left[R_s - G_{epi} R_s^{Cd} F_{Cd}\right] \quad (1)$$

where g_T is the correction for departure from the 1/v cross section behavior of the monitor isotope and G_{th} and G_{epi} are the thermal and epithermal neutron self-shielding factors, respectively. R_s and R_s^{Cd} are the reaction rates per atom for bare and cadmium-covered foil irradiations. F_{Cd} is the cadmium correction factor for the monitor isotope of interest. For the calculation of thermal component, Eq. (1) is simply expressed as follows:

$$\Phi_{th} = 1.128 \times \Phi_0 \quad (2)$$

In Eq. (2), the multiplier 1.128 is used for the relation of total equivalent 2,200 m/s flux. In other words, all thermal neutrons are assumed to be at an energy of 0.0253 eV [14]. The epithermal component of neutron flux, Φ_{epi}, is defined as:

$$\Phi_{epi} = \Phi_0 \cdot \frac{1}{(R_{Cd} - 1)} \cdot \frac{g_T \sigma_0}{I_0} \cdot \frac{G_{th}}{G_{epi}} \quad (3)$$

The reaction rate per atom for bare foil, R_s, and cadmium covered foil, $R_{s,Cd}$, irradiation can be derived from the induced activity in the foil [15,16].

For the determination of neutron flux, the foils used have high purity of 99.95%, a 0.0508-mm (0.002 inch) thickness, and a 12.7-mm (0.5 inch) diameter. They were purchased from Shieldwerx, A Division of Bladewerx LLC, Rio Rancho, NM, USA. The mean values, thermal neutron self-shielding factor $G_{th} = 0.939(5)$, and epithermal neutron self-shielding factor $G_{epi} = 0.257(4)$ were calculated for the foils based on the formulae given in [15,17]. Nuclear and decay data required for the ^{197}Au(n,γ)^{198}Au reaction are provided in Table 1.

3. Results and discussion

In a radiotherapy treatment room, the contribution of a photoneutron dose to patients due to a therapeutic photon beam from an 18-MV linac operating in photon mode was measured using gold activation foils. Some were placed in the solid water phantom (RW3) layers and the others suspended freely on the walls of the room. The collimator was opened to specify a 20 × 20 cm^2 X-ray field size and each irradiation session lasted for about 12.5 minutes to obtain a total 50 Gy photon dose at $d_{max} = 5$ cm below the surface of the phantom placed at the isocenter. The measured neutron fluxes for different

Table 2 – Neutron flux measurements and corresponding dose equivalents in solid water phantom.

Phantom depth (cm)	Thermal neutron flux, Φ (n/cm^2/s)	Epithermal neutron flux, Φ(n/cm^2/s)	Neutron dose equivalent[a] (mSv)
0	(6.65 ± 0.20) × 10^5	(1.15 ± 0.05) × 10^5	7.45 ± 0.41
5	(3.73 ± 0.11) × 10^6	(1.12 ± 0.05) × 10^5	33.56 ± 1.82
10	(2.18 ± 0.06) × 10^6	(3.73 ± 0.17) × 10^4	19.17 ± 1.04

[a] Fluence-to-dose conversion factors, $H_{p,slab}$ (10,0°)/ϕ are taken from International Commission on Radiological Protection publication 74 [24].

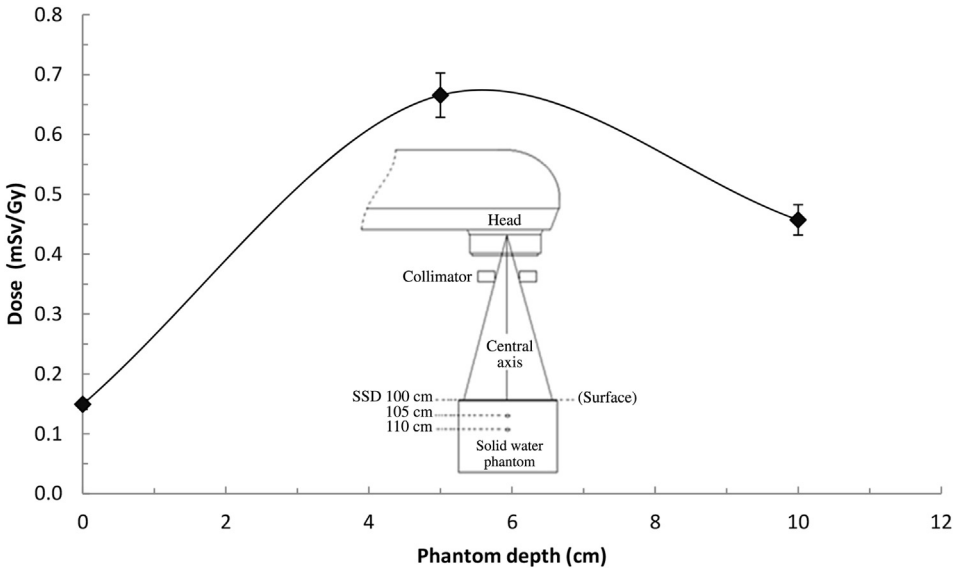

Fig. 3 – Variation of photo-neutron dose equivalent to the given photon dose depending on depth of phantom placed at isocenter.

depths in the solid water phantom are given in Table 2. Fluence (ϕ) was calculated from the measured flux (Φ) by taking into account exposure time (t_{irr}). Then, personal dose equivalent and ambient dose equivalent values were determined from the resulting thermal neutron fluences by employing the neutron fluence-to-dose conversion factors as $H_{p,slab}(10,0^{\circ})/\phi$ and $H^{*}(10)/\phi$ at a thermal neutron energy of ~0.0253 eV, which was taken from The International Commission on Radiological Protection 74 document [24]. Similarly, the doses due to epithermal neutron fluences were calculated using the average conversion factors in the epithermal neutron energy range from ~0.5 eV to 100 keV. If we express the neutron dose equivalent in terms of mSv per Gy photon dose, it is observed that the maximum total neutron contamination is below $d_{max} = 5$ cm depth from phantom surface. Thus, the corresponding total dose equivalent due to thermal plus epithermal neutrons was found to be about 0.67 ± 0.04 mSv per Gy photon dose at a 5-cm depth in the water phantom, where the maximum cumulative photon dose is 50.4 ± 0.6 Gy at the isocenter with a 20 × 20 cm^2 X-ray field size. The dose distribution depending on depth in the phantom is also shown in Fig. 3. The increase in neutron contamination dose is expected due to not only the increased thermal flux in the water phantom but also the maximum photon flux (thus leading to the increment in photo-neutron dose) measured at the treatment planning depth from the phantom surface, where the depth is theoretically assumed to be $d_{max} = 5$ cm from the surface of solid water phantom.

Table 3 – Measured neutron fluxes and calculated dose equivalent values in treatment room, maze entrance, and operator room.

Irradiation location	Total neutron flux[b] Φ (n/cm^2/s)	Neutron dose (mSv)
Patient position at isocenter at $d_{max} = 5$ cm in the phantom[a]	(3.85 ± 0.21) × 106	33.56 ± 1.82
Left wall (~3.8 m distance from isocenter), foil D suspended	(1.00 ± 0.03) × 10^5	0.80 ± 0.03
Right wall (~3.8 m distance from isocenter), foil E suspended	(9.81 ± 0.30) × 10^4	0.78 ± 0.02
Patient position 45cm distance from isocenter, foil F suspended	(1.32 ± 0.04) × 10^5	1.05 ± 0.03
Maze wall-1 (foil G suspended)	(1.24 ± 0.06) × 10^4	0.098 ± 0.005
Maze wall-2 (foil H suspended)	(1.07 ± 0.52) × 10^3	(8.47 ± 4.08) × 10^{-3}
Maze entrance (foil I suspended)	(2.36 ± 1.30) × 10^2	(1.87 ± 1.03) × 10^{-3}
Operator room (foil J suspended)	(3.06 ± 2.88) × 10^2	(2.43 ± 2.28) × 10^{-3}

[a] Two set foils denoted to A, B, and C are co-irradiated as bare foil and with cadmium cover-foil between phantom layers.
[b] Due to only thermal neutron plus epithermal neutron flux, where excepting the fast neutrons with energies of above 500 keV.

For other locations in the treatment room, the ambient dose equivalent values, $H^{*}(10)$, due to thermal plus epithermal neutrons are given in Table 3. For instance, the total neutron contamination dose in the operator room was found to be almost zero, i.e., the value of 2.43 ± 2.28 μSv. The photo-neutron dose was measured to be 33.56 ± 1.82 mSv at the patient position (phantom surface) at the isocenter, where surface-to-source distance = 100 cm was chosen.

The calculated neutron dose values for the points represented by letters D and E, as marked in Fig. 1, were expected to be the same due to the symmetrical distances from the left and right primary barriers but some scattering arising from the variation of distances to the ceiling and floor had some effect. The neutron doses measured at the entrance door

Table 4 – A comparison of the measured neutron fluence and corresponding neutron dose for 10-MV, 15-MV, and 18-MV linacs.

Medical accelerator	Measurement/ calculation method[a]	Potential (MV)	Field size (cm^2)	Neutron fluence per unit photon dose ($n/cm^2/Gy$)	Neutron dose to photon dose (mSv/Gy)	Total neutron per unit photon dose (n/Gy)	Reference
Varian Clinac DHX	Au-foil	18	20 × 20	$(5.71 \pm 0.33) \times 10^7$	0.67 ± 0.04	$(2.28 \pm 0.13) \times 10^{10}$	This work
Varian 2100 C/D	PC films	18	20 × 20	None	3.30 ± 0.50	None	Hashemi et al 2011 [25]
Varian CLINAC 2100C	CR39 dosimeter	18	20 × 20	1.07×10^5	1.15	None	Paredes et al 1999 [26]
Mevatron-77	Au foil	18	15 × 15	2.30×10^5	None	5.18×10^7	Palta et al 1984 [8]
Philips SL/75-20	In-foil	18	10 × 10	1.40×10^6	None	1.40×10^8	Gur et al 1978 [27]
Elekta Precise	Au-foil	18	None	$(9.11 \pm 0.19) \times 10^6$	1.95	None	Esposito et al 2008 [28]
Varian 21EX Platinum Plus	BSS/TLD	18	10 × 10	$(5.00 \pm 0.40) \times 10^6$	None	5.00×10^8	Vega-Carrillo et al 2010 [29]
Varian Clinac 2100/2300C	Monte Carlo	18	None	None	None	1.20×10^{12}	Kase et al 1998 [30]
Varian Clinac 21EX	BSS/Au-foil	18	10 × 10	7.47×10^6	1.65	7.47×10^8	Kry et al 2008 [31]
Siemens	Monte Carlo	18	20 × 20	None	6.96	None	Chibani et al 2003 [32]
Siemens	Monte Carlo	18	10 × 10	None	5.03	None	Chibani et al 2003 [32]
Varian	Monte Carlo	18	10 × 10	None	20.40	None	Chibani et al 2003 [32]
Varian	Monte Carlo	15	10 × 10	None	13.30	None	Chibani et al 2003 [32]
Varian Clinac 2300C/D	Bubble Detector	15	20 × 20	None	2.50	None	Ipe et al 2000 [33]
Varian Clinac 2300C/D	Au-foil	15	20 × 20	None	3.00	None	Ipe et al 2000 [33]
Varian Clinac 2300C/D	Track-Etch	15	20 × 20	None	8.50	None	Ipe et al 2000 [33]
Elekta Precise	CR39 dosimeter	15	15 × 15	$(6.10 \pm 0.12) \times 10^6$	None	1.37×10^9	Khaled et al 2011 [34]
Varian 23EX	CR39 dosimeter	15	15 × 15	$(5.23 \pm 0.10) \times 10^6$	None	1.18×10^9	Khaled et al 2011 [34]
Varian CLINAC 21EX	In-foil	15	20 × 20	1.97×10^5	None	7.88×10^7	Liu et al 2011 [7]
Varian CLINAC 21EX	In-foil	10	20 × 20	1.46×10^4	None	5.84×10^6	Liu et al 2011 [7]
Elekta Precise	CR39 dosimeter	10	15 × 15	$(4.00 \pm 0.08) \times 10^6$	None	9.00×10^8	Khaled et al 2011 [34]
Neptun 10PC	Monte Carlo	10	20 × 20	None	0.042	None	Zabihinpoor et al 2011 [35]
Varian Clinac 2100/2300C	Monte Carlo	10	None	None	None	3.80×10^{10}	Kase et al 1998 [30]

BSS, bonner sphere spectrometer; TLD, thermoluminescent dosimeter.
[a] Surface-to-source distance = 100 cm.

(letter I) and in the operator room (letter J) were also found to be very low, i.e., almost zero.

As given in Table 4, the total neutron fluence was measured to be 5.71×10^7 n/cm^2 per Gy-photon dose at the isocenter. This measured fluence and the corresponding photo-neutron dose were compared with the results obtained in literature at different X-ray field sizes (10×10 cm^2, 15×15 cm^2, and 20×20 cm^2) from other 10-, 15-, and 18-MV linacs. It is clear that a relatively higher fluence is estimated in our work than those other studies. This is due to the contribution of the epithermal neutron component to the thermal component in the water phantom. In general, the contamination neutron dose equivalent was determined to be < 0.7% of the photon dose delivered to the patient at the isocenter. Nevertheless, this extra dose delivered to patients due to photo-neutrons in the vicinity of the patient position is not a negligible fraction of the therapeutic photon dose. Thus, this implies that there is a need for dose reduction measures from the point of view of radiation protection during the treatment of patients.

This study presents a measurement method of photo-neutron dose employing the gold foil activation method. It is a fact that during operation of a medical linac in photon mode, the production of photo-neutrons via (γ,n) reactions from the target and surrounding materials is not negligible because of the high-energy photon beams used in radiotherapy. In a

water phantom, the measured neutron dose equivalents as a function of depth per unit total photon dose were presented for 20 × 20 cm^2 X-ray fields. In all cases the measured maximum neutron dose equivalent was less than 0.7% of the photon dose.

Since the gold foil activation technique is a more reliable and effective method of measuring both thermal and epithermal neutron fluence rates, the neutron doses were accurately assessed at the patient position. The present results indicate that the total neutron dose equivalent represents a small contribution to the therapeutic photon dose, meaning that it is still two or three orders of magnitude smaller than the photon dose delivered to the patient. However, the amount of this extra dose in the vicinity of the patient position cannot be neglected in view of radiological protection assessment related to the patients. In conclusion, there is a need for dose reduction measures against the neutron contamination. For instance, some elastomeric materials loaded with neutron absorbers might be used as protective aprons during the treatment of patients.

Conflicts of interest

All authors have no conflicts of interest to declare.

Acknowledgments

This work was supported by the Ankara University Scientific Research Project, No. BAP-12A4045001.

REFERENCES

[1] A. Alfuraih, M. Chin, N. Spyrou, Measurements of the photonuclear neutron yield of 15 MV medical linear accelerator, J. Radioanal. Nucl. Chem. 278 (2008) 681–684.
[2] International Commission on Radiological Protection (ICRP 103), The 2007 Recommendations of the International Commission on Radiological Protection, ICRP Publication 103, Ann. ICRP, Elsevier Ltd., The Netherlands, 2007.
[3] C. Ongaro, A. Zanini, U. Nastasi, J. Ródenas, G. Ottaviano, C. Manfredotti, Analysis of photoneutron spectra produced in medical accelerators, Phys. Med. Biol. 45 (2000) L55.
[4] A. Nath, A. Boyer, P. La Riviere, R. McCall, K. Price, Neutron measurements around high energy X-ray radiotherapy machine, The American Association of Physicists in Medicine (AAPM), 1986. Report No. 19.
[5] R. Barquero, R. Mendez, H.R. Vega-Carrillo, M.P. Iñiguez, T.M. Edwards, Neutron spectra and dosimetric features around an 18 MV linac accelerator, Health Phys. 88 (2005) 48–58.
[6] R.B. Sanz, R.M. Villafañe, M. Bayo, H. Vega-Carrilho, Determination of neutron dose to patients from a 18 MV LINAC, Trabajo CB/UEN-07/039, 2001.
[7] W.S. Liu, S.P. Changlai, L.K. Pan, H.C. Tseng, C.Y. Chen, Thermal neutron fluence in a treatment room with a Varian linear accelerator at a medical university hospital, Rad. Phys. Chem. 80 (2011) 917–922.
[8] J.R. Palta, K.R. Hogstrom, C. Tannanonta, Neutron leakage measurements from a medical linear accelerator, Med. Phys. 11 (1984) 498.
[9] PTW [Internet]. [cited 2014 May 6] PTW Freiburg GmbH, Germany. Available from: http://www.ptw.de/acrylic_and_rw3_slab_phantoms0.html.
[10] H. Yücel, A.N. Solmaz, E. Köse, D. Bor, Spectral interference corrections for the measurement of ^{238}U in materials rich in thorium by a high resolution γ-ray spectrometry, Appl. Rad. Isot. 67 (2009) 2049–2056.
[11] S. Jovanovic, A. Dlabac, N. Mihaljevic, ANGLE v2.1—New version of the computer code for semiconductor detector gamma-efficiency calculations, Nucl. Instrum. Meth. Res. A 622 (2010) 385–391.
[12] O. Sima, D. Arnold, C. Dovlete, GESPECOR: a versatile tool in gamma-ray spectrometry, J. Radioanal. Nucl. Chem. 248 (2001) 359–364.
[13] M. Karadag, H. Yücel, Thermal neutron cross-section and resonance integral for $^{164}Dy(n,\gamma)^{165}Dy$ reaction", Nucl. Instrum. Meth. Res. A 550 (2005) 626–636.
[14] ASTM E261, Standard practice for determining neutron fluence, fluence rate, and spectra by radioactivation techniques, Annual Book of American Society for Testing Materials (ASTM) standards 12.02, 2010, pp. 40–49.
[15] M. Karadag, H. Yücel, Measurement of thermal neutron cross-section and resonance integral for ^{186}W (n, γ)^{187}W reaction by the activation method using a single monitor, Ann. Nucl. Energy 31 (2004) 1285–1297.
[16] H. Yücel, H. Karadag, Measurement of thermal neutron cross section and resonance integral for $^{165}Ho(n, \gamma)^{166g}Ho$ reaction by the activation method, Ann. Nucl. Energy 32 (2005) 1–11.
[17] K.H. Beckurts, K. Wirtz, Neutron Physics, Springer, New York, 1964.
[18] V. Kolotov, F. De Corte, Compilation of k_0 and related data for Neutron Activation Analysis (NAA) in the form of an electronic database, Pure Appl. Chem. 76 (2004) 1921–1925.
[19] T. El Nimr, F. De Corte, L. Moens, A. Simonits, J. Hoste, Epicadmium neutron activation analysis (ENAA) based on the k_0-comparator method, J. Radioanal. Nucl. Chem. 67 (1981) 421–435.
[20] J.K. Tuli, Nuclear wallet cards, 2011.
[21] LARA Database [Internet]. Nucléide Gamma and Alpha Library, [cited 2014 October 24]. Available: from http://laraweb.free.fr.
[22] M.J. Berger, J.H. Hubbell, S.M. Seltzer, J. Chang, J.S. Coursey, R. Sukumar, D.S. Zucker, K. Olsen, XCOM: Photon Cross Section Database (version 1.5) [Internet]. National Institute of Standards and Technology, Gaithersburg, MD, 2010 [cited 2014 May 15]. Available from: http://physics.nist.gov/xcom.
[23] GESPECOR Software [Internet]. [cited 2014 March 15]. Available from: http://www.gespecor.de/en.
[24] International Commission on Radiological Protection, Conversion coefficients for use in radiological protection against external radiation, ICRP Publication 74, Ann. ICRP 26 (1996) 159–205.
[25] S.M. Hashemi, G. Raisali, M. Taheri, A. Majdabadi, M. Ghafoori, The effect of external wedge on the photoneutron dose equivalent at a high energy medical linac, Nukleonika 56 (2011) 49–51.
[26] L. Paredes, R. Genis, M. Balcazar, L. Tavera, E. Camacho, Fast neutron leakage in 18 MeV medical electron accelerator, Rad. Measurements 31 (1999) 475–478.
[27] D. Gur, J.C. Rosen, A.G. Bukovitz, A.W. Gill, Fast and slow neutrons in an 18-MV photon beam from a Philips SL/75-20 linear accelerator, Med. Phys. 5 (1978) 221–222.
[28] A. Esposito, R. Bedogni, L. Lembo, M. Morelli, Determination of the neutron spectra around an 18MV medical LINAC with a passive Bonner sphere spectrometer based on gold foils and TLD pairs, Rad. Measurements 43 (2008) 1038–1043.

[29] H.R. Vega-Carrillo, B. Hernandez-Almaraz, V.M. Hernandez-Davila, A. Ortiz-Hernandez, Neutron spectrum and doses in a 18 MV LINAC, J. Radioanal. Nucl. Chem. 283 (2010) 261–265.
[30] K.R. Kase, X.S. Mao, W.R. Nelson, J.C. Liu, J.H. Kleck, M. Elsalim, Neutron fluence and energy spectra around the Varian Clinac 2100C/2300C Medical Accelerator, Health Phys. 74 (1998) 38–47.
[31] S.F. Kry, R.M. Howell, U. Titt, M. Salehpour, R. Mohan, O.N. Vassiliev, Energy spectra, sources, and shielding considerations for neutrons generated by a flattening filter-free Clinac, Med. Phys. 35 (2008) 1906–1911.
[32] O. Chibani, C.M. Ma, Photonuclear dose calculations for high-energy photon beams from Siemens and Varian linacs, Med. Phys. 30 (2003) 1990–2000.
[33] N.E. Ipe, S. Roesler, S. Jiang, C. Ma, Neutron measurements for intensity Modulated Radiation therapy. Paper presented at the Engineering in Medicine and Biology Society, Proceedings of the 22nd Annual International Conference of the IEEE, 2000.
[34] N. Khaled, E. Attalla, H. Ammar, W. Khalil, Dosimetry and fast neutron energies characterization of photoneutrons produced in some medical linear accelerators, Radiat. Eff. Defect. S. 166 (2011) 908–917.
[35] S. Zabihinpoor, M. Hasheminia, Calculation of neutron contamination from medical linear accelerator in treatment room, Adv. Studies Theor. Phys. 5 (2011) 421–428.